Published OnlineFirst August 11, 2009; DOI: 10.1158/1535-7163.MCT-09-0107

Xenogeneic immunization with human tyrosine hydroxylase DNA vaccines suppresses growth of established neuroblastoma

Nicole Huebener,[1] Stefan Fest,[3] Kerstin Hilt,[2] Alexander Schramm,[4] Angelika Eggert,[4] Tahir Durmus,[1] Anja Woehler,[1] Alexander Stermann,[1] Matthias Bleeke,[1] Bianca Baykan,[1] Silke Weixler,[1] Gerhard Gaedicke,[1] and Holger N. Lode[1]

Departments of [1]Pediatrics, Experimental Oncology, Campus Virchow-Klinikum and [2]Dermatology and Allergy, Allergy Center Charité, Charité-University Medicine Berlin, Berlin, Germany; [3]Pediatric Immunotherapy, University Children's Hospital, Otto-von-Guericke-Universität Magdeburg, Magdeburg, Germany; and [4]Department of Pediatric Hematology and Oncology, University of Essen, Essen, Germany

Abstract

Neuroblastoma (NB) is a challenging malignancy of the sympathetic nervous tissue characterized by a very poor prognosis. One important marker for NB is the expression of tyrosine hydroxylase (TH), the first-step enzyme of catecholamine biosynthesis. We could show stable and high TH gene expression in 67 NB samples independent of the clinical stage. Based on this observation, we addressed the question of whether xenogeneic TH DNA vaccination is effective in inducing an anti-NB immune response. For this purpose, we generated three DNA vaccines based on pCMV-F3Ub and pBUD-CE4.1 plasmids encoding for human (h)THcDNA (A), hTH minigene (B), and hTHcDNA in combination with the proinflammatory cytokine interleukin 12 (C), and tested prophylactic and therapeutic efficacy to suppress primary tumor growth and spontaneous metastasis. Here we report that xenogeneic TH DNA vaccination was effective in eradicating established primary tumors and inhibiting metastasis. Interestingly, this effect could not be enhanced by adding the Th1 cytokine interleukin 12. However, increased IFN-γ production and NB cytotoxicity of effector cells harvested from vaccinated mice suggested the participation of tumor-specific CTLs in the immune response. The depletion of $CD8^+$T cells completely abrogated the hTH vaccine–mediated anti-NB immune response. Furthermore, rechallenging of surviving mice resulted in reduced primary tumor growth, indicating the induction of a memory immune response. In conclusion, xenogeneic immunization with TH-derived DNA vaccines is effective against NB, and may open a new venue for a novel and effective immunotherapeutic strategy against this challenging childhood tumor. [Mol Cancer Ther 2009;8(8):2392–401]

Introduction

Neuroblastoma (NB) is the most common extracranial solid tumor in childhood. Despite the introduction of new treatment strategies, including blood stem cell transplantation, differentiation therapy with retinoic acid, and passive immunotherapy with anti-GD2 antibodies, the long-term survival rate, especially of stage 4 NB patients, remains poor, ranging from 35% to 40% (1, 2). This emphasizes the need for effective adjuvant treatment strategies, which also involve the induction of an effective cellular anti-NB immune response.

NB, like many other malignancies, escape early immune surveillance by down-regulation of MHC class I expression (3, 4) or decrease in the production of lymphocyte-attracting chemokines, such as CCL2 (5). However, MHC class I antigen expression can be restored in NB cells within an inflammatory environment and become accessible for the cellular arm of the immune system (6). In fact, Morandi et al. were able to detect NB-specific CTLs in the blood of NB patients (7), showing that immunotherapy approaches, which induce an active CTL-mediated immune response, might be suitable for treatment.

A major obstacle in active immunotherapy for malignant disease is to overcome tolerance against self-antigens expressed by tumor tissue. Two objectives are crucial to achieve this goal: (*a*) the choice of a suitable antigen and (*b*) an effective vaccination strategy. The choice of antigen is limited by the nature of the tumor because it should be either tumor-specific (e.g., prostate specific antigen; refs. 8, 9) or tumor-associated (10, 11). With regard to the application method, the strategies are manifold, and differ in efficacy and handling. The most common vaccination strategies used for cancer patients up to now are peptide vaccinations with the use of either directly injected peptide formulations (12), or administration of peptide-pulsed or tumor lysate–pulsed donor-derived dendritic cells (7, 13). A more novel approach is the application of DNA plasmid vaccines, which have the advantages of high versatility and stability, and which also stimulate toll-like receptor 9

Received 3/4/09; revised 5/6/09; accepted 5/18/09; published OnlineFirst 8/11/09.

Grant support: Emmy-Noether-Programm of the Deutsche Forschungsgemeinschaft (Lo635/2) and the Fördergesellschaft Kinderkrebs-Neuroblastom-Forschung e.V.

The costs of publication of this article were defrayed in part by the payment of page charges. This article must therefore be hereby marked *advertisement* in accordance with 18 U.S.C. Section 1734 solely to indicate this fact.

Requests for reprints: Holger N. Lode, Department of Pediatrics, Experimental Oncology, Campus Virchow Klinikum, Charité-University Medicine Berlin, Augustenburger Platz 1, Berlin 13353, Germany. Phone: 49-30-450-666233; Fax: 49-30-450-566916. E-mail: holger.lode@charite.de

Copyright © 2009 American Association for Cancer Research.

doi:10.1158/1535-7163.MCT-09-0107

Downloaded from mct.aacrjournals.org on January 16, 2021. © 2009 American Association for Cancer Research.

Published OnlineFirst August 11, 2009; DOI: 10.1158/1535-7163.MCT-09-0107

(14). DNA vaccines can be injected directly into the muscle (15), given by electroporation or gene gun (16), or after transfection of dendritic cells, which ensures the production of the antigen of choice directly inside professional antigen-presenting cells (17). A fourth possibility is the oral application of DNA vaccines delivered by live attenuated bacteria, like *Salmonella typhimurium*, which are rapidly taken up by antigen-presenting cells of the gastrointestinal tract. This strategy provides for a proinflammatory milieu by signaling through toll-like receptors and subsequently mediate a danger signal (18).

In earlier experiments with a syngeneic NB mouse model, we could show that tyrosine hydroxylase (TH) is a suitable NB-associated antigen for DNA vaccination. In fact, murine TH-derived DNA vaccines were found to induce a CTL-mediated and NB-directed immune response in mice (19, 20). However, in contrast to preclinical mouse data, immune responses achieved in humans with syngeneic DNA vaccines are often disappointing, emphasizing the fact that results from animal models cannot be easily transferred to the human system (21). Nevertheless, several strategies are available to enhance DNA vaccine–induced immune responses in the patient. Thus, earlier studies showed that xenogeneic DNA vaccines not only induce immune responses against the "foreign" protein but also generate autoreactive CTLs that recognize the homologous host protein by cross-priming (12, 22). The mechanism underlying this phenomenon is probably based on the generation of so-called heteroclitic epitopes from the sequence of the xenogeneic protein. Here, peptides are generated during proteasomal degradation that differ from the host sequence in certain amino acid positions, which are important for binding into the groove of host MHC molecules. This may lead to a higher binding affinity to MHC molecules compared with the host epitopes, resulting in a stronger stimulation of T-cell receptors (23, 24).

Another possibility for enhancing antitumor immune responses induced by DNA vaccines is the introduction of costimulatory molecules into the coding sequence of the DNA vaccine plasmid (e.g., cytokines or chemokines; refs. 25, 26).

In the present study, we determined that TH is stably and highly expressed in 67 human NBs independent of the disease stage. This finding supports the hypothesis that TH is a suitable target antigen for anti-NB immunotherapy. Based on this observation, we are the first to investigate the effect of two xenogeneic TH-based DNA vaccines in a syngeneic NB mouse model, and to compare their efficacy in the presence and absence of the proinflammatory cytokine interleukin (IL)-12. Interestingly, stable monoubiquitination of the hTH DNA vaccines, which is mediated by the expression plasmid pCMV-F3Ub, in combination with attenuated *S. typhimurium* as vaccine vehicle, induces the most effective anti-NB immunity that could not be further enhanced by the addition of IL-12. Furthermore, we could show that the immune response is mediated by CTLs. Finally, the hTH DNA proved to be effective in a therapeutic vaccination setting, resulting in a memory response as indicated by protection against a lethal rechallenge with tumor cells.

Materials and Methods

Determination of *TH* Expression in NB Patients

TH expression was detected as described previously (27). Briefly, a cohort of 67 primary NBs profiled with the use of Affymetrix Gene Arrays was reanalyzed for expression of *TH*. Expression of *TH* was correlated to clinicopathologic variables with the use of one-way ANOVA (Fig. 1).

Design and Construction of DNA Vaccines

Three different DNA vaccines were designed: vaccines A and B based on the mammalian ubiquitin expression plasmid pCMV-F3Ub, kindly provided by Lindsay Whitton and Fernando Rodriguez, The Scripps Research Institute, La Jolla, CA (20, 28); and vaccine C based on pBUD-CE4.1 (= vaccine C; Invitrogen). Vaccine A encodes for the cDNA sequence of hTH (pCMV-hTHcDNA). Vaccine B encodes for a DNA minigene comprising the three major hTH-derived MHC class I epitopes in our mouse model (pCMV-hTH3; Fig. 2A and B), whereas in vaccine C, the sequences of hTH cDNA and single-chain IL-12 (scIL-12) are expressed by two independent expression units (Fig. 2A; pBUD-hTH–IL-12).

The cDNA sequence of hTH isoform 2 was amplified by PCR: (*a*) for pCMV-F3Ub with the use of primers hTH-pCMV-up (GAAGATCTTCATGCCCACCCCCGACGCCA-CCACGCCACAG), including a *Bgl*II, and hTH-pCMV-down (CCCTTGCCCATGCGC-TGAGTGCCATTGGCTAG-GAATTCAGATCTTC), including *Bgl*II and *Eco*RI restriction sites; and (*b*) for pBUD-CE4.1 with the use of primers hTH-pBUD-up (ACGCGTCGACATGC-CCACCCCC-GACGCCACCACGCCACAG), including a *Sal*I, and hTH-pBUD-down (cgggatccaTAGCCAATGGCACT-CAGCGCATGGGCAAGGG), including a *Bam*HI restriction site. Amplification was carried out under the following PCR conditions: 95°C for 30 s, 68°C for 45 s, and 72°C for 3 min running over 22 cycles.

The hTH3 minigene was constructed by overlapping reverse transcription-PCR as described previously (20). The minigene design included separation of each epitope by an AAY spacer sequence for each of the constructs, which was shown to be a preferential proteasomal cleavage site (ref. 29; Fig. 2B). Furthermore, a HA tag was added at the 3′ end to show peptide expression. Vaccines A and B were cloned into the mammalian expression vector pCMV-F3Ub with the use of a *Bgl*II restriction site downstream of mutated ubiquitin (A76; ref. 28).

The sequence for scIL-12 encoding for the two subunits of IL-12, p35 and p40 separated by a $(Gly_4Ser)_3$ linker (30), was subcloned into pBUD-CE4.1 with the use of *Xho*I and *Kpn*I restriction sites. For this purpose, the scIL-12 fragment was amplified by PCR with the use of the primers scIL-12–pBUD-up (ggggtacccatgagtgtgcccactcagg-tcctggggttgctg) and scIL-12–pBUD-down (ccgctcgagtag-gatcggaccctgcagggaacacatgccc), and the following PCR conditions: 95°C, 30 s; 63°C, 45 s; 72°C, 90 s; 22 cycles.

Downloaded from mct.aacrjournals.org on January 16, 2021. © 2009 American Association for Cancer Research.

Published OnlineFirst August 11, 2009; DOI: 10.1158/1535-7163.MCT-09-0107

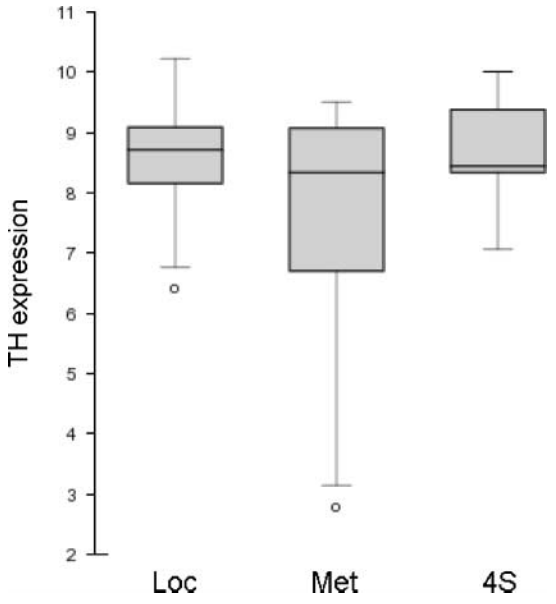

Figure 1. Expression of *TH* in NB. Gene expression of TH was determined in 67 human NB samples and correlated with tumor spread in a box plot. *Y-axis*, log values of *TH* expression. Localized tumors (Loc), stages 1 and 2 ($n = 39$); metastatic tumors (Met), stages 3 and 4 ($n = 19$); stage 4S ($n = 9$). One-way ANOVA for differential *TH* expression between Loc and Met tumors, $P = 0.1$.

Protein Expression Analysis

The expression of hTH protein was tested after transient transfection of the DNA vaccines into CHO-1 cells with the use of the Metafectene transfection reagent (Biontex Laboratories) according to the manufacturer's protocol. After 24 or 48 h, cells were lysed (0.1% SDS in PBS, pH 7.4, 4°C, 30 min) and centrifuged (10,000 g, 4°C, 45 min). Lysates were analyzed by SDS-PAGE with the use of the Novex system (Invitrogen). Proteins were blotted onto a nitrocellulose membrane (Amersham). Blots were blocked with blocking buffer (5% milk, 0.1% Tween 20, PBS, pH 7.4) and incubated with anti-hTH antibody (diluted 1:33 in blocking buffer; Vector Laboratories). Peroxidase-labeled anti-mouse IgG antibody (Sigma) was added (1:1,000 in blocking buffer). The membrane was washed (thrice, 15 min, room temperature, 0.1% Tween 20, PBS), and signals were analyzed with the ECL Detection Reagents (Amersham).

Lymphoblast Proliferation Assay

To test the activity of IL-12 (p70), encoded by the vector design of pBUD-hTH–scIL-12, supernatants from vector-transfected CHO-1 cells were used in a lymphoblast proliferation assay, in which activated lymphoblasts produce IFN-γ upon stimulation with IL-12. Briefly, human peripheral blood mononuclear cells were isolated from peripheral blood of a healthy donor by Ficoll density centrifugation. Peripheral blood mononuclear cells were cultured for 3 d at a concentration of 5×10^5/mL in RPMI 1640–based (PAA Laboratories) tissue culture medium [10 mmol/L HEPES (Gibco), 0.006% (w/v) L-arginin-monohydrochloride (Sigma), 0.1% (w/v) dextrose (Sigma), 5% human AB serum (Cambrex), 100 μg/mL penicillin-streptomycin (Invitrogen)]. For lymphoblast activation, 20 μg/mL phytohemagglutinin P (Sigma) and 50 IU/mL IL-2 were added. Activated lymphoblasts (50 μL) in a concentration of 4×10^5 cells/mL were added in triplicates to each well of a 96-well plate. Supernatants (50 μL) from CHO-1 cells transfected with pBUD-hTH–scIL-12 were added 48 h after transfection. Recombinant IL-12 (BD Pharmingen) applied at different concentrations and supernatants from mock-transfected CHO-1 cells were used as positive and negative controls, respectively. Plates were incubated at 37°C and with 5% CO_2. After 48 h, supernatants were taken, and the amount of IFN-γ produced by lymphoblasts was measured by ELISA (human IFN-γ ELISA set; BD Pharmingen). From these results, a standard curve of IL-12 concentration–dependent IFN-γ production was generated. Specific IL-12 bioactivity of vector-encoded scIL-12 was calculated from this standard curve.

DNA Vaccine Delivery

Attenuated *S. typhimurium* strain SL7207 (AroA-), kindly provided by Dr. Bruce A. D. Stocker, Stanford University School of Medicine, Stanford, CA, were used for *in vivo* vaccination experiments as described previously (20). Briefly, a single SL7207 colony was grown in Luria-Bertani medium, and mid-log phase bacteria were washed twice with ice-cold water. Bacterial cells (1×10^8) were admixed with 0.5 μg of plasmid DNA. Electroporation was done in the Eppendorf Multiporator at 2 kV, 25 μF, and 200 Ω for 0.5 s. Cells were immediately covered with 600 μL SOC medium (Invitrogen) and incubated for 45 min at 37°C. A sample of 100 μL was plated onto Luria-Bertani plates containing 50 μg/mL ampicillin (Sigma). Resistant colonies containing the DNA vaccines were cultured and stored after confirmation of the DNA sequence. Mice ($n = 6$-8) were immunized by oral gavage of SL7207 bacteria in mid-log growth phase carrying the vaccines and control plasmids.

Cells and Mice

NXS2 murine NB (31) and CHO-1 cells were grown in high-glucose DMEM or RPMI 1640, respectively (PAA Laboratories). All media were supplemented with 10% FCS (PAA Laboratories) and 100 μg/mL penicillin-streptomycin (Invitrogen). Syngeneic female A/J mice were obtained at 8 to 10 wk of age from Harlan-Winkelmann. The NXS2 model was used as previously described (31). Briefly, primary tumors were induced by s.c. injection of 2×10^6 NXS2 cells in serum-free DMEM (day 0), and primary tumor growth was analyzed by microcaliper measurements. The tumor volume was calculated according to 1/2width × length × width. When primary tumors reached a volume of 500 mm^3 on average and/or showed signs of necrosis, they were surgically removed and their weights determined. Spontaneous metastasis was determined at indicated time points after removal of primary tumors by measurements of liver weights, counts of metastatic nodules on the liver and other organ surfaces, and scoring the metastatic load according to 0% = 0, <20% = 1, 20%-50% = 2, and >50% = 3. In the long-term therapeutic survival experiment, s.c. primary tumors were removed

Downloaded from mct.aacrjournals.org on January 16, 2021. © 2009 American Association for Cancer Research.

Published OnlineFirst August 11, 2009; DOI: 10.1158/1535-7163.MCT-09-0107

individually when they reached a volume of 500 mm^3 or showed signs of necrosis or ulceration, in contrast to the prophylactic vaccination described above. Two vaccinations (5×10^8 salmonella per mouse) were done on days 3 and 8 after s.c. tumor cell injection. A boost was given 2 wk after tumor removal, adjusted individually to the day of surgery (marked as days 30-50 in Fig. 3A). Survivor mice received a rechallenge with 2×10^6 NXS2 cells on day 87 without receiving any further vaccinations. At this time point, new naïve and mock control mice entered the study (each $n = 6$) and were also challenged with the same dosage of NXS2 cells. This was followed by two vaccinations 4 and 9 d after tumor cell injection in the mock control group. Secondary s.c. tumor growth (rechallenge) was determined over the next 14 d and compared with tumor growth of the new controls (Fig. 3A).

T cells were depleted *in vivo* with the use of anti-CD8 (53-6.7) antibody (BD Pharmingen) as previously described (32). Briefly, depletion of $CD8^+$T cells was accomplished by i.p. injection of anti-CD8 (200 μg) on days −1, 7, and 14.

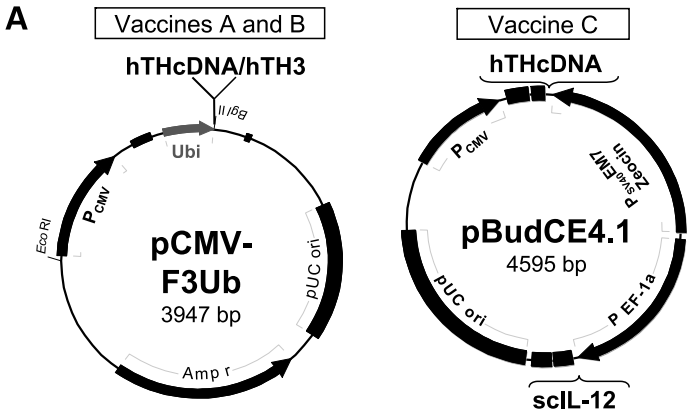

B

	Sequence	*syfpeithi* score
hTH3	epi1: FETFEAKI	24
	epi2: FDPYTLAI	20
	epi3: LDKCHHLV	18

epi 1 AAY epi 2 AAY epi 3 AAY HA-tag

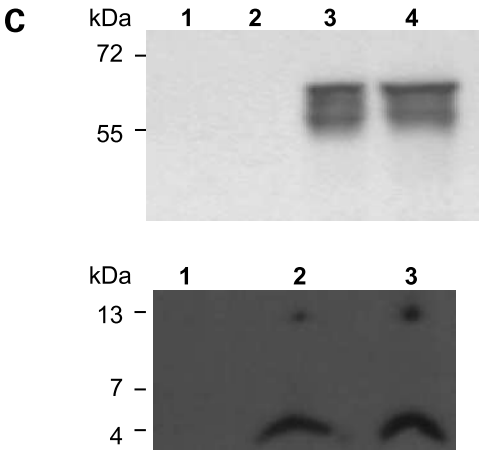

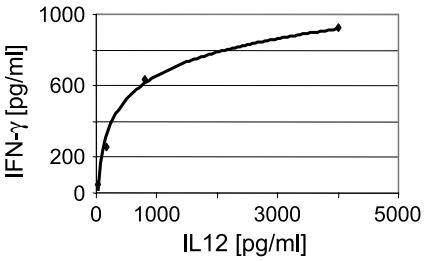

pBUD	IL12 [pg/ml]	IFNγ [pg/ml]	bioactive IL12 [pg/ml]	Bio-activity in %
scIL12-hTH	3000	447,5	326,3	**9,2**
	1500	297,5	146,8	**10,2**
mock		18,0	33,2	
		31,9	35,7	

Figure 2. Vector design and expression of encoded antigens. Schematic of the two mammalian vector backbones used in this study (**A**). For vaccines A and B, the plasmid pCMV-F3Ub encoding for Ubi-Ala76 upstream of the *Bgl*II cloning site leading to the expression of a stably monoubiquitinated protein was used. Both the full-length hTHcDNA sequence and the hTH3 DNA minigene were subcloned with the use of the *Bgl*II restriction site. Vaccine C was constructed with the use of pBudCE4.1 equipped with two independent expression units driven by the CMV and EF-1α promoter, respectively. The sequences of scIL-12 and hTHcDNA were subcloned into pBudCE4.1 with the use of restriction sites *Xho*I and *Kpn*I, as well as *Sal*I and *Bam*HI as indicated. Design of the hTH3 minigene (**B**). The selection of the hTH epitopes was accomplished as previously described (20) by using the MHC class I epitope prediction software SYFPEITHI. Additionally, the binding scores according to SYFPEITHI are shown. A HA tag was included at the 3′ end to allow detection in western blots. Expression analysis of vaccines A to C after transient transfection of CHO-1 cells (**C**). Protein expression was determined after 10% to 14% gradient SDS-PAGE and blotting onto a nitrocellulose membrane 24 or 48 h after transfection of CHO-1 cells. Expression of hTH (59 kDa) was analyzed with an anti-TH antibody (*top*). *Lane 1*, untransfected control; *lane 2*, pBud mock control; *lane 3*, hTHcDNA–scIL-12; *lane 4*, hTHcDNA). The detection of the hTH3 minigene (4.8 kDa) was accomplished with anti-HA antibody after 24 (*lane 2*) and 48 h (*lane 3*). Mock-transfected CHO-1 cells were used as a negative control (*lane 1*). Determination of the specific mIL-12 bioactivity of the scIL-12 construct in supernatants from transfected CHO-1 cells (**D**). For this purpose, a bioassay measuring the ability of the construct to induce IFN-γ was used (*top*). The bioactivity was compared with that of a standard mIL-12.

Downloaded from mct.aacrjournals.org on January 16, 2021. © 2009 American Association for Cancer Research.

Published OnlineFirst August 11, 2009; DOI: 10.1158/1535-7163.MCT-09-0107

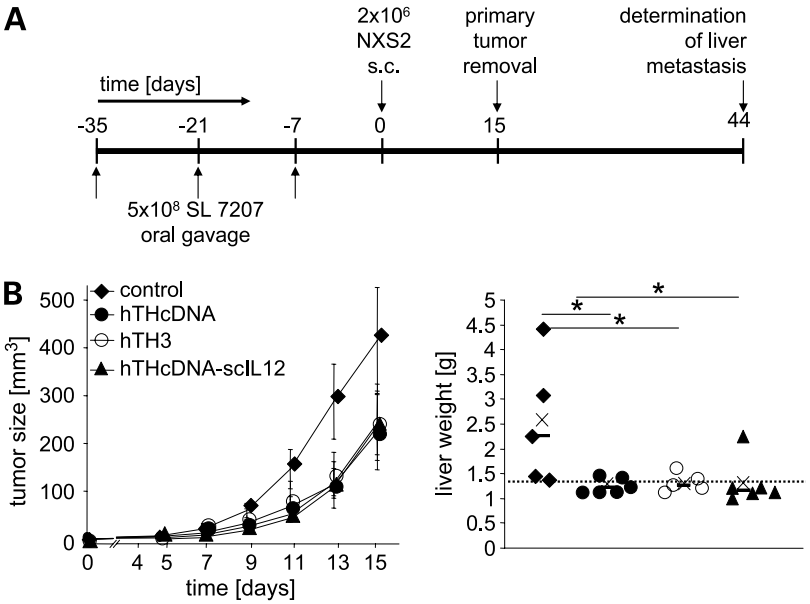

Figure 3. Anti-NB immune response induced by xenogeneic TH DNA vaccines. Schematic of prophylactic vaccination (**A**). Three oral vaccinations with 5×10^8 plasmid-bearing attenuated *S. typhimurium* (SL7207) were applied at 2-wk intervals into A/J mice ($n = 6$). Tumor cell injection (2×10^6 NXS2 neuroblastoma cells s.c.), primary tumor removal, and determination of liver metastasis were done at indicated time points. Primary tumor growth was measured for a period of 15 d until surgical tumor removal (**B**) by microcaliper measurements. The primary tumor sizes were calculated as $1/2 \times \text{width}^2 \times \text{length}$. Values, mean ± SE ($n = 6$) of tumor sizes in cubic millimeters. Spontaneous liver metastasis was determined by measurements of liver weights of fresh specimen (**C**). Results, mean ± SE (*, $P \leq 0.05$). *Horizontal line*, normal liver weights of mice without metastases (1.2-1.4 g). Metastatic score of livers at the end of the *in vivo* experiment: 0% = 0, <20% = 1, 20-50% = 2, >50% = 3.

C

	number of tumor nodes on liver surface	grade of liver metastasis
control	250, 250, 15, 12, 10	3, 3, 2, 1, 1
hTHcDNA	0, 0, 0, 0, 0, 5	0, 0, 0, 0, 0, 1 (p<0.05)
hTH3	0, 0, 0, 5, 6	0, 0, 0, 1, 1 (p<0.05)
hTH-scIL12	0, 0, 3, 3, 4, 100	0, 0, 1, 1, 1, 3

All animal experiments were done according to the German guide for the care and use of laboratory animals (i.e., Tierschutzgesetz). Animal experiments were repeated at least once, and the data shown are representative results from one experiment.

Immunohistochemistry

Infiltration of primary tumors by T cells was analyzed by immunohistochemistry with the use of anti-CD8 antibody (53-6.7) and anti-CD4 antibody (RM4-5; BD Pharmingen) as previously described (32). The average number of infiltrating T cells was quantified by light microscopy analyzing 10 high power fields at a magnification of ×400.

Cytotoxicity Assay

At indicated time points, splenocytes were harvested and incubated for 5 d in the presence of 30 Gy-irradiated NXS2 NB cells in RPMI 1640 [10% FCS, 100 μg/mL penicillin-streptomycin, 50 μmol/L β-mercaptoethanol (Sigma), 100 U/mL IL-2] at a ratio of 100:1. NXS2 NB served as target cells. CTL activity was determined with the use of a standard ^{51}Cr release assay. Briefly, 2×10^6 target cells were labeled (2 h, 37°C) with 0.5 mCi ^{51}Cr (1 mCi/mL sodium chromate; Perkin Elmer) in a total volume of 2 mL and washed thrice with complete DMEM. Target cells were plated out at 5,000 cells per well in a 96-well plate. Effector cells were added to triplicate wells at varying effector to target cell ratios. Samples were taken after 4 and 8 h of incubation, and released radioactivity was determined in a gamma counter (1470 Wizard, Wallace; Perkin Elmer). Maximum release was induced by incubation of labeled target cells with 5 μL of a 10% SDS solution. Cytotoxicity was calculated according to lysis (%) = [experimental release (cpm) − spontaneous release (cpm)]/[maximum release (cpm) − spontaneous release (cpm)] × 100 (%).

IFN-γ ELISA

IFN-γ concentrations were measured to assess the activation of T cells in the splenocyte population upon incubation with NXS2 target cells. Briefly, 1×10^4 irradiated NXS2 cells were cultured with freshly isolated splenocytes from vaccinated or control mice at an E:T ratio of 100:1 in RPMI 1640 [10% FCS, 100 μg/mL penicillin-streptomycin, 50 μmol/L β-mercaptoethanol (Sigma), 100 U/mL IL-2]. On days 3, 4, and 5, supernatants were collected, and an IFN-γ ELISA was done according to the manufacturer's protocol (murine IFN-γ ELISA set; BD Pharmingen).

Statistics

The statistical significance of differential findings between experimental groups was determined by nonparametric Kruskal-Wallis test and further analyzed by Mann-Whitney *U* test. Primary tumor growth data after

Downloaded from mct.aacrjournals.org on January 16, 2021. © 2009 American Association for Cancer Research.

Published OnlineFirst August 11, 2009; DOI: 10.1158/1535-7163.MCT-09-0107

therapeutic vaccination were analyzed by χ^2 test. In all cases, differences were considered significant at $P < 0.05$.

Results

Expression of TH in Human NB Tissue

We first investigated the mRNA expression of *TH* by reanalysis of Affymetrix expression profiling data in a cohort of 67 primary NB. *TH* expression was found to be high in 66 of 67 samples without significant correlation of *TH* expression with stage international neuroblastoma staging system or clinical outcome. Interestingly, although *TH* expression is proposed as a marker for minimal residual disease, no significant difference was found for *TH* expression between localized and metastatic tumors (Fig. 1).

Design and Characterization of hTH DNA Vaccines

The design of hTH full-length DNA vaccines is based on pCMVF3Ub and pBudCE4.1 vectors (Fig. 2A). The minigene was selected by screening of the hTH sequence for three peptides with high affinity to MHC class I (H2K-k), each separated by an AAY spacer (Fig. 2B). The expression of full-length human TH gene and hTH3 minigenes encoded by DNA vaccines A, B, and C was shown by western blots after transient transfection of CHO-1 cells (Fig. 2C). The hTH protein (59 kDa) was detected in CHO-1 cells 48 h after transfection (*top*) both from the pBUD and the pCMV plasmids, respectively (Fig. 2C, *top*, *lanes 3* and *4*). Similarly, the hTH3 minigene expression was shown as indicated by a peptide signal at 4.8 kDa 24 and 48 h after transfection (Fig. 2C, *bottom, lanes 2* and *3*).

Bioactivity of pBUD-encoded scIL-12

The bioactivity of pBUD-encoded scIL-12 was determined with a lymphoblast proliferation assay with the production of IFN-γ as a readout for IL-12 activity (Fig. 2D). We could clearly show the release of IFN-γ from lymphoblasts incubated with supernatant from CHO-1 cells transfected with pBUD-hTH–scIL-12 in contrast to mock-transfected controls, indicating bioactivity of the scIL-12 construct (Fig. 2D). The specific bioactivity was calculated based on scIL-12 protein concentration and the amount of IFN-γ produced, which indicated that the scIL-12 construct revealed a specific IL-12 bioactivity of 10%. This is lower than previously reported (30), possibly due to a different IL-12 standard and the use of human instead of murine lymphoblasts in the bioassay.

Prophylactic Effect of hTH DNA Vaccines against Primary Tumor Growth and Spontaneous Liver Metastases

All three DNA vaccine constructs were tested in a prophylactic vaccination setting after oral vaccine delivery with the use of live attenuated *S. typhimurium* SL7207 as a vaccine carrier in the syngeneic NXS2 NB mouse model (Fig. 3A). Both the hTH cDNA and the hTH3 minigene DNA vaccine encoded by the ubiquitin vector pCMV induced a 50% reduction of primary tumor growth and prevented liver metastasis in the majority of animals (Fig. 3B and C). The pBUD vaccine encoding for both hTH and scIL-12 did not further enhance the antitumor immune response (Fig. 3B and C).

Mechanisms Involved in the Anti-NB Immune Response Induced by hTH DNA Vaccination

To determine whether there is a contribution by $CD8^+$ effector T cells in the hTH-mediated anti-NB immune response, we depleted $CD8^+$T cells *in vivo* in the prophylactic vaccination setting, followed by a lethal challenge with NXS2 NB cells. Depletion of $CD8^+$T cells completely abrogated protective immunity induced by hTH DNA vaccination in contrast to controls (Fig. 4). Furthermore, splenocytes from the pCMV-hTHcDNA group lysed NXS2 target cells in a cytotoxicity assay in contrast to effector cells from mock-vaccinated control mice (Fig. 5A). We could also show that splenocytes from mice vaccinated with hTHcDNA and hTH3 minigene are activated upon incubation with NXS2 target cells, resulting in a 10-fold and 7-fold increase of the Th1 cytokine IFN-γ, respectively, compared with control splenocytes (Fig. 5B). These findings were further supported by the analysis of infiltrating $CD8^+$ and $CD4^+$T cells into primary tumor tissue by immunohistochemistry. We show a

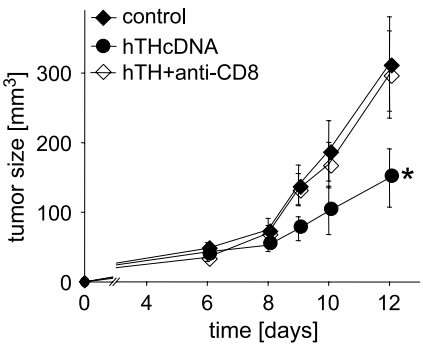

	Metastatic scores	tumor-free mice
control	3, 2, 2, 2, 1, 0	1
hTHcDNA	2, 0, 0, 0, 0	4
hTH + antiCD8	3, 3, 3, 3, 2, 2, 0	1

Figure 4. Determination of the tumor load (primary tumor and metastases) of mice depleted of $CD8^+$ T cells *in vivo*. Mice ($n = 6$) were depleted of $CD8^+$T cells by i.p. injection of anti-CD8 antibody (clone 53-6.7) as described in Materials and Methods. Groups of mice were immunized according to the prophylactic vaccination scheme shown in Fig. 3A and challenged by s.c. injection of 2×10^6 NXS2 neuroblastoma cells. Primary tumor growth was measured for a period of 12 d until surgical tumor removal by microcaliper measurements (*left*). The primary tumor sizes were calculated as $1/2 \times \text{width}^2 \times \text{length}$. Values, mean ± SE ($n = 6$) of tumor sizes in cubic millimeters. Disseminated metastasis of all mouse organs was scored at the end of the *in vivo* experiment (*right*): 0% = 0, <20% = 1, 20-50% = 2, >50% = 3 (*left*). *Right column*, numbers of mice free of primary tumor and metastases.

Downloaded from mct.aacrjournals.org on January 16, 2021. © 2009 American Association for Cancer Research.

Published OnlineFirst August 11, 2009; DOI: 10.1158/1535-7163.MCT-09-0107

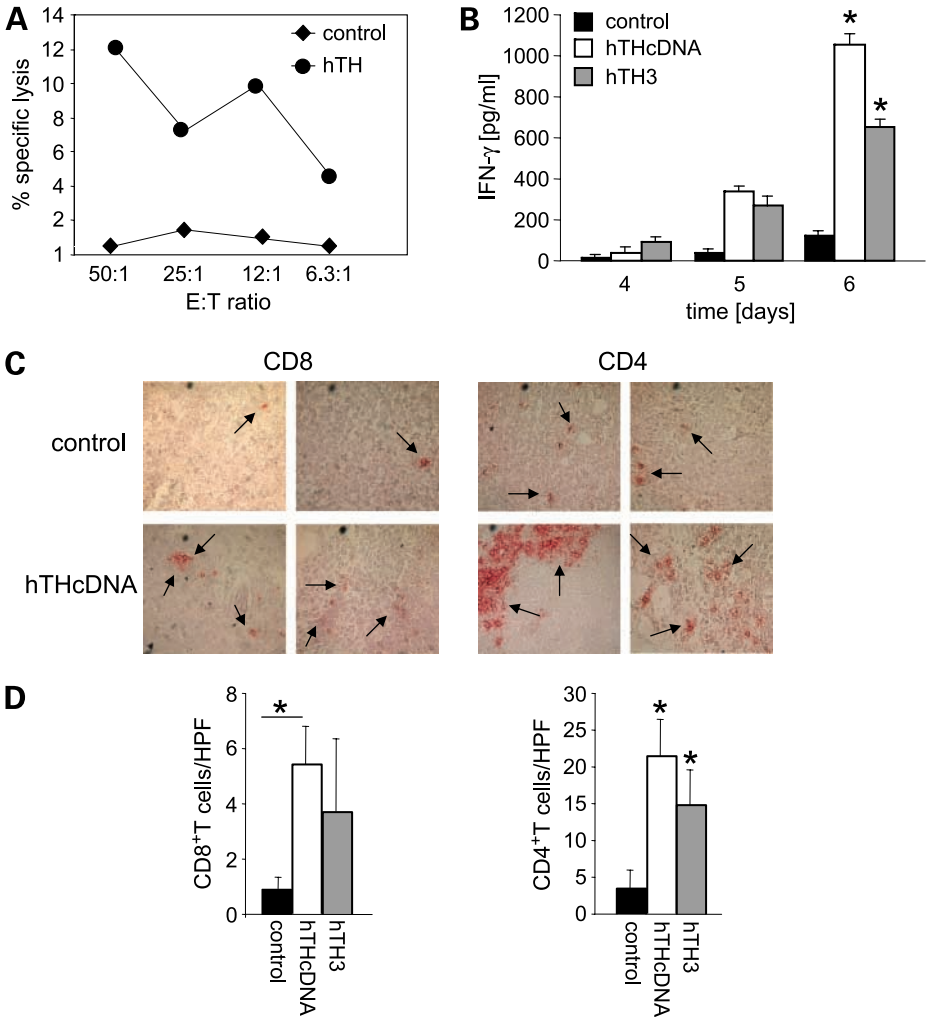

Figure 5. The induction of NB-specific CTLs after immunization with xenogeneic TH DNA vaccines. Splenocytes harvested from immunized and control mice were stimulated for 5 d in the presence of irradiated NXS2 cells as outlined in Material and Methods, and used in cytotoxicity (**A**) and T-cell activation assays (**B**). NXS2 target cells were loaded with ^{51}Cr (**A**). Effector cells from hTHcDNA-vaccinated and control mice were added at distinct effector to target cell ratios in triplicates. Percent cytotoxicity was calculated as indicated in Materials and Methods. Results, mean ± SD. T-cell activation was determined by release of IFN-γ over time measured by ELISA 3, 4, and 5 d after stimulation with irradiated NXS2 cells (**B**). Results, mean of triplicates ± SD. Infiltration of tumor tissue by $CD8^+$ and $CD4^+$ T cells was analyzed by immunohistochemistry (**C** and **D**). For this purpose, frozen sections of primary tumors were stained with anti-CD8 and anti-CD4 antibodies. Red staining (*black arrows*) indicates infiltration by $CD8^+$ and $CD4^+$ T cells, respectively (**C**). The number of CD8+ and CD4+ T cells per high power field was analyzed by light microscopy (**D**). Ten fields at ×400 magnification were counted. *Bars*, means ± SD ($n = 10$). The differences between groups of mice receiving the hTH3 (*light gray*) and hTHcDNA (*white*) vaccines, and all control groups (*black*) were statistically significant (*, $P < 0.05$).

5-fold increase of infiltrating $CD8^+$T cells in the hTHcDNA-pCMV group, and a 7-fold and 5-fold increase of infiltrating $CD4^+$Tcells for hTHcDNA for hTH3 groups (Fig. 5C and D). In summary, these data suggest primarily a $CD8^+$T-cell–mediated antitumor response.

Therapeutic Effect of Xenogeneic Vaccination (hTHcDNA) *In vivo*

To determine therapeutic efficacy, mice with established primary tumors were immunized with the hTHcDNA-pCMV vaccine by oral gavage at the indicated time points (Fig. 6A). Mice receiving the hTHcDNA-pCMV vaccine showed a primary tumor rejection in 50% of mice (Fig. 6B and C). This finding was in contrast to control mice suffering from systemic metastases before day 87 (data not shown), including one mouse that failed to develop a primary tumor but died on day 68 due to severe organ metastasis (Fig. 6B).

The three surviving mice were rechallenged with a lethal dose of NXS2 cells, resulting in a reduction of primary tumor growth rate and weight in contrast to naïve controls or mice receiving the empty vector (Fig. 6D). In summary, these data show the therapeutic efficacy of the xenogeneic hTH DNA vaccination translating into long-lasting anti-NB immunity.

Discussion

The application of DNA vaccines encoding for tumor-associated antigens is a promising approach for cancer immunotherapy. However, many preclinically successful DNA vaccines lead to disappointing results after application in human trials (21, 33). This can partly be explained by the differences in the expression pattern of toll-like receptor 9, which is responsible for the recognition of CpG motifs included in bacterial plasmid DNA backbone (34). In humans, toll-like receptor 9 expression is limited to B cells and plasmacytoid dendritic cells, in contrast to mice in which most of the preclinical studies are done. In this species, B cells, monocytes, and probably all subsets of dendritic cells express toll-like receptor 9 (35, 36). Consequently, antitumor effects in mice induced by DNA vaccines are not necessarily transferable to humans. However, DNA vaccination effects can be further

Downloaded from mct.aacrjournals.org on January 16, 2021. © 2009 American Association for Cancer Research.

Published OnlineFirst August 11, 2009; DOI: 10.1158/1535-7163.MCT-09-0107

enhanced by using xenogeneic DNA, encoding for highly homologous proteins that are foreign to the species to be vaccinated (37, 38).

TH is the first-step enzyme of catecholamine biosynthesis and, consequently, limited in its expression in nonneuronal tissue. We could show by microarray analysis that *TH* is highly and stably expressed independent of disease stage in 67 human NBs. This result, together with the fact that syngeneic vaccination with murine TH DNA vaccines induces efficient anti-NB immune responses in mice without provoking autoimmunity (20), strongly supports our hypothesis that TH is a suitable target antigen for anti-NB immunotherapy.

Here we tested the anti-NB activity of xenogeneic vaccination with the use of an hTH cDNA vaccine in a syngeneic NB mouse model and determined whether it is possible to further enhance the antitumor immune response by adding the sequence of a costimulatory cytokine to the vector design. Additionally, we planned to verify our previous data by developing a rationally designed hTH-derived minigene encoding for three MHC class I epitopes that were chosen from the MHC class I epitope prediction database SYFPEITHI.

In both prophylactic and therapeutic vaccination settings, the xenogeneic hTH vaccines effectively induced an anti-NB immune response. This immune response was mediated by CTLs as shown by *in vitro* assays and by depletion of $CD8^+$T cells *in vivo* (Figs. 4 and 5). We also found an increased $CD4^+$T cell infiltrate in tumors of hTH-vaccinated mice in contrast to controls (Fig. 5). This result, together with the fact that tumor-surviving mice developed immunity after

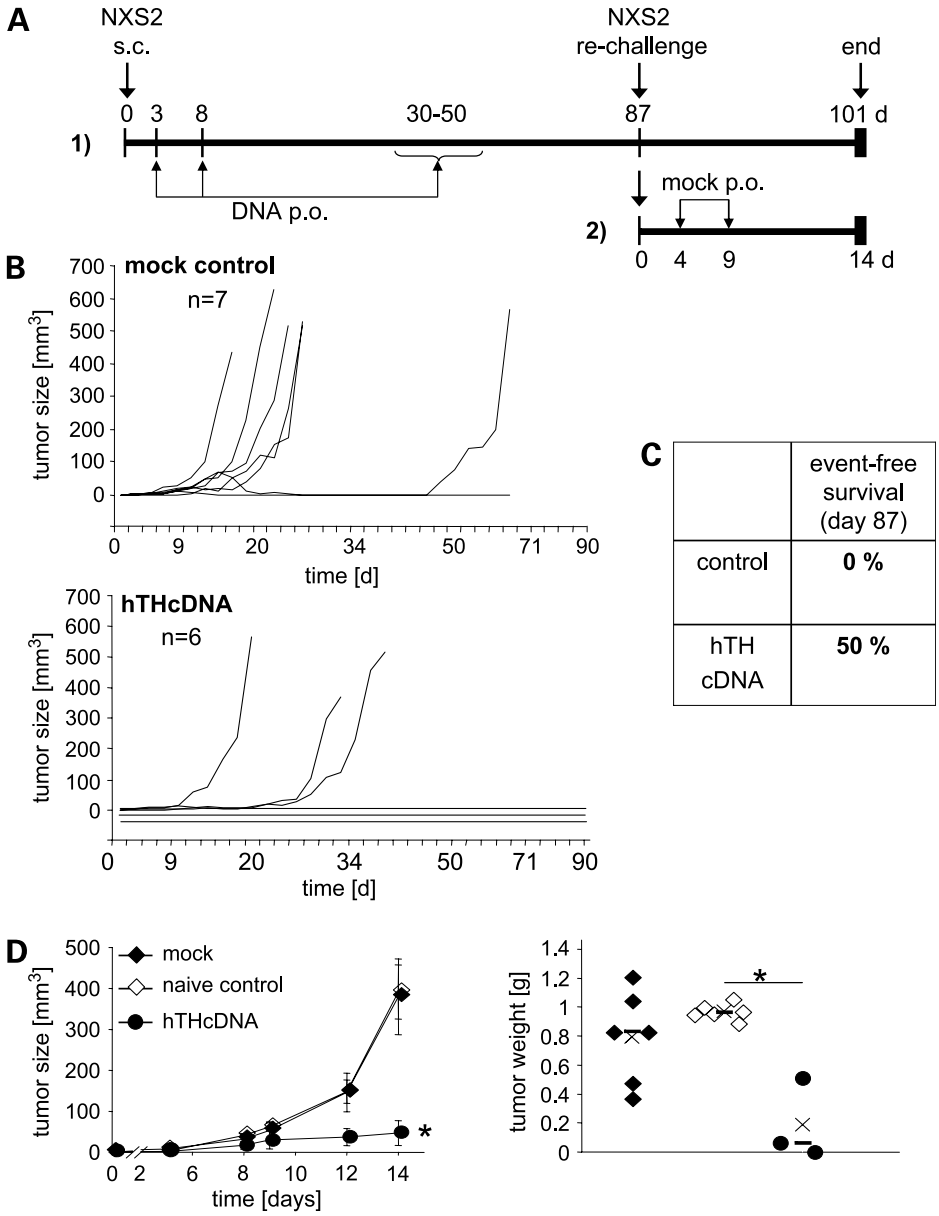

Figure 6. Therapeutic vaccination against NB with the hTHcDNA vaccine. Schematic of oral therapeutic DNA immunization against NB (**A**). Mice were immunized with pCMV mock ($n = 7$) and pCMV-hTHcDNA ($n = 6$; ref. 1) 3 d after s.c. injection of 2×10^6 NXS2 NB cells when primary tumors were established (5×10^8 salmonella per mouse). Primary tumors were surgically removed when their sizes exceeded 500 mm^3. A boost vaccination was carried out 2 wk after tumor removal (5×10^8 salmonella per mouse), adjusted individually to the day of surgery of each mouse. Surviving mice were rechallenged by s.c. injection of 2×10^6 NXS2 on day 87. Tumor growth in these rechallenged mice was compared with naïve and mock controls, of which new mice entered the study on day 87 (each $n = 6$); mock controls received two vaccinations with empty plasmid-bearing salmonella 4 and 9 d after tumor challenge (5×10^8 salmonella per mouse; ref. 2). Tumor growth was determined by microcaliper measurements (**B**) in mock-vaccinated (*top*) and hTHcDNA-vaccinated (*bottom*) mice. The primary tumor sizes were calculated as 1/2 × width^2 × length. The differences in numbers of absent primary tumors between experimental groups of animals were analyzed at the end of the experiment (day 68) by χ^2 test (*, $P \leq 0.05$). Determination of the percentage of mice remaining free of NB (primary tumor and metastases; **C**). Analysis of primary tumor growth in surviving and control mice (**D**). Primary tumor growth was measured for a period of 14 d until surgical tumor removal by microcaliper measurements (*left*). The primary tumor sizes were calculated as 1/2 × width^2 × length. Values, mean ± SE ($n = 6$) of tumor sizes in cubic millimeters (*left*). The tumor weight was determined at the end of the experiment (*right*). Differences between experimental groups of animals were analyzed by Mann-Whitney *U* test (*, $P \leq 0.05$).

Downloaded from mct.aacrjournals.org on January 16, 2021. © 2009 American Association for Cancer Research.

Published OnlineFirst August 11, 2009; DOI: 10.1158/1535-7163.MCT-09-0107

a lethal rechallenge with tumor cells (Fig. 6), not only confirms our previous data with the use of syngeneic murine TH DNA vaccination (20) but further indicates a role for $CD4^+$T-cell help in inducing and maintaining immunologic memory (39).

Additionally, the hTH3 minigene was equally effective as the hTH cDNA vaccine, supporting the concept of rationally designing suitable DNA vaccines by epitope prediction in a species-independent manner. However, full-length vaccines have the advantage of providing for the whole range of possible MHC class I epitopes for all haplotypes in humans. Nevertheless, customized DNA vaccine design for patients remains particularly interesting and applicable when the tumor-associated antigen of choice is potentially hazardous (40).

In a variety of preclinical xenogeneic DNA vaccination experiments, the encoded foreign antigen induced autoantibodies (41, 42), which contributed to the antitumor immune responses. Therefore, we tested mouse sera taken at different time points after vaccination for the presence of anti-TH antibodies, which were not detectable by ELISA (data not shown), indicating that in our system a humoral response plays a subordinate role.

IL-12 plays a key role in the differentiation and homeostasis of effector and memory $CD8^+$T cells (43). Furthermore, this cytokine supports antitumor immunity because it is able to augment $CD8^+$T cell avidity toward tumor targets (44) and also is essential for shifting $CD4^+$T cells into a Th1 phenotype (45). Because the TH DNA vaccines are delivered by attenuated *S. typhimurium*, processing occurs inside of professional antigen-presenting cells in the Peyer's patches (46). Therefore, we hypothesized that the simultaneous expression of the proinflammatory cytokine IL-12 and TH in this location would enhance the activation and stimulation of antigen-specific $CD8^+$T cells. However, in contrast to others, we were not able to enhance the antitumor efficacy of our DNA vaccine by adding the sequence of IL-12 into the DNA plasmid design. This might be attributed to the different application method of IL-12. In fact, many other studies showed the positive effects of intratumoral IL-12 injection (47) or of using genetically engineered IL-12–producing tumor cells as a vaccine (30). Importantly, the results obtained in our *in vivo* studies led us to the conclusion that our DNA vaccine design, including a mutated ubiquitin tag (pCMVF3Ub; vaccines A and B; Fig. 2), provides for an equally efficient immune response. The crucial importance of mutated ubiquitin in this respect has already been shown in the past and is probably the reason for the induction of a very effective MHC class I antigen epitope presentation after proteasomal degradation in the antigen-presenting cells after oral vaccination with vaccine-carrying attenuated *S. typhimurium* (20). Besides, it could be shown by others that hypomethylated CpG motives, which are included in our bacterial plasmid DNA, effectively induce IL-12 secretion by dendritic cells (48), thereby providing comparable costimulatory conditions. However, the costimulatory effects of additional cytokine sequences to provoke a Th1-directed immune response should not be underestimated or ignored for the application of DNA vaccines in humans (49).

In summary, after evaluation of syngeneic DNA vaccination with the NB-associated antigen TH, we could prove the efficacy of xenogeneic DNA vaccination with TH-derived DNA against NB *in vivo*. The immune response induced is mediated by NB-specific CTLs and provides antitumor immunity protecting mice from a lethal rechallenge with NB. In other *in vivo* studies in our laboratory, we found that the combination of tagging the tumor-associated antigen with Ubi-Ala76 and attenuated bacteria as vaccine vehicles is much more effective against NB than delivery by gene gun.[5] We conclude from our experience over the past years that a combination of attenuated bacteria as vaccine vehicles with stable monoubiquitination of the tumor-associated antigen mediated by the vaccine vector provides the most promising and practicable possibility to induce effective antitumor immune responses in NB.

Disclosure of Potential Conflicts of Interest

No potential conflicts of interest were disclosed.

Acknowledgments

We thank Ralph A. Reisfeld for critical review and discussion of the manuscript.

References

1. Pritchard J, Cotterill SJ, Germond SM, et al. High dose melphalan in the treatment of advanced neuroblastoma: results of a randomised trial (ENSG-1) by the European Neuroblastoma Study Group. Pediatr Blood Cancer 2005;44:348–57.

2. Volchenboum SL, Cohn SL. Progress in defining and treating high-risk neuroblastoma: lessons from the bench and bedside. J Clin Oncol 2009; 27:1003–4.

3. Murphy C, Nikodem D, Howcroft K, Weissman JD, Singer DS. Active repression of major histocompatibility complex class I genes in a human neuroblastoma cell line. J Biol Chem 1996;271:30992–9.

4. Raffaghello L, Prigione I, Bocca P, et al. Multiple defects of the antigen-processing machinery components in human neuroblastoma: immunotherapeutic implications. Oncogene 2005;24:4634–44.

5. Song L, Ara T, Wu HW, et al. Oncogene MYCN regulates localization of NKT cells to the site of disease in neuroblastoma. J Clin Invest 2007;117:2702–12.

6. Drew PD, Lonergan M, Goldstein ME, et al. Regulation of MHC class I and β 2-microglobulin gene expression in human neuronal cells. Factor binding to conserved cis-acting regulatory sequences correlates with expression of the genes. J Immunol 1993;150:3300–10.

7. Morandi F, Chiesa S, Bocca P, et al. Tumor mRNA-transfected dendritic cells stimulate the generation of CTL that recognize neuroblastoma-associated antigens and kill tumor cells: immunotherapeutic implications. Neoplasia 2006;8:833–42.

8. Gregor PD, Wolchok JD, Turaga V, et al. Induction of autoantibodies to syngeneic prostate-specific membrane antigen by xenogeneic vaccination. Int J Cancer 2005;116:415–21.

9. Marshall DJ, San Mateo LR, Rudnick KA, et al. Induction of Th1-type immunity and tumor protection with a prostate-specific antigen DNA vaccine. Cancer Immunol Immunother 2005;54:1082–94.

10. Palomba ML, Roberts WK, Dao T, et al. CD8+ T-cell-dependent immunity following xenogeneic DNA immunization against CD20 in a tumor challenge model of B-cell lymphoma. Clin Cancer Res 2005;11:370–9.

11. Rosenberg SA, Yang JC, Schwartzentruber DJ, et al. Immunologic

[5] S. Fest, unpublished data.

Downloaded from mct.aacrjournals.org on January 16, 2021. © 2009 American Association for Cancer Research.

Published OnlineFirst August 11, 2009; DOI: 10.1158/1535-7163.MCT-09-0107

and therapeutic evaluation of a synthetic peptide vaccine for the treatment of patients with metastatic melanoma. Nat Med 1998;4:321–7.

12. Loftus DJ, Castelli C, Clay TM, et al. Identification of epitope mimics recognized by CTL reactive to the melanoma/melanocyte-derived peptide MART-1(27-35). J Exp Med 1996;184:647–57.

13. von Euw EM, Barrio MM, Furman D, et al. A phase I clinical study of vaccination of melanoma patients with dendritic cells loaded with allogeneic apoptotic/necrotic melanoma cells. Analysis of toxicity and immune response to the vaccine and of IL-10-1082 promoter genotype as predictor of disease progression. J Transl Med 2008;6:6–20.

14. Liu MA, Wahren B, Karlsson Hedestam GB. DNA vaccines: recent developments and future possibilities. Hum Gene Ther 2006;17:1051–61.

15. Tu CF, Lin CC, Chen MC, et al. Autologous neu DNA vaccine can be as effective as xenogenic neu DNA vaccine by altering administration route. Vaccine 2007;25:719–28.

16. Wang S, Zhang C, Zhang L, et al. The relative immunogenicity of DNA vaccines delivered by the intramuscular needle injection, electroporation and gene gun methods. Vaccine 2008;26:2100–10.

17. Yang S, Vervaert CE, Burch J, Jr., et al. Murine dendritic cells transfected with human GP100 elicit both antigen-specific CD8(+) and CD4(+) T-cell responses and are more effective than DNA vaccines at generating anti-tumor immunity. Int J Cancer 1999;83:532–40.

18. Matzinger P. An innate sense of danger. Ann N Y Acad Sci 2002;961:341–2.

19. Huebener N, Lange B, Lemmel C, et al. Vaccination with minigenes encoding for novel 'self' antigens are effective in DNA-vaccination against neuroblastoma. Cancer Lett 2003;197:211–7.

20. Huebener N, Fest S, Strandsby A, et al. A rationally designed tyrosine hydroxylase DNA vaccine induces specific antineuroblastoma immunity. Mol Cancer Ther 2008;7:2241–51.

21. Wolchok JD, Yuan J, Houghton AN, et al. Safety and immunogenicity of tyrosinase DNA vaccines in patients with melanoma. Mol Ther 2007;15:2044–50.

22. Weber LW, Bowne WB, Wolchok JD, et al. Tumor immunity and autoimmunity induced by immunization with homologous DNA. J Clin Invest 1998;102:1258–64.

23. Dyall R, Bowne WB, Weber LW, et al. Heteroclitic immunization induces tumor immunity. J Exp Med 1998;188:1553–61.

24. Speiser DE, Baumgaertner P, Voelter V, et al. Unmodified self antigen triggers human CD8 T cells with stronger tumor reactivity than altered antigen. Proc Natl Acad Sci U S A 2008;105:3849–54.

25. Elzaouk L, Pavlovic J, Moelling K. Analysis of antitumor activity elicited by vaccination with combinations of interleukin-12 DNA with gp100 DNA or the chemokine CCL21 *in vivo*. Hum Gene Ther 2006;17:859–70.

26. Luo Y, Zhou H, Mizutani M, et al. A DNA vaccine targeting Fos-related antigen 1 enhanced by IL-18 induces long-lived T-cell memory against tumor recurrence. Cancer Res 2005;65:3419–27.

27. Zeng Y, Huebener N, Fest S, et al. Fractalkine (CX3CL1)- and interleukin-2-enriched neuroblastoma microenvironment induces eradication of metastases mediated by T cells and natural killer cells. Cancer Res 2007;67:2331–8.

28. Rodriguez F, Zhang J, Whitton JL. DNA immunization: ubiquitination of a viral protein enhances cytotoxic T-lymphocyte induction and antiviral protection but abrogates antibody induction. J Virol 1997;71:8497–503.

29. Holzhutter HG, Frommel C, Kloetzel PM. A theoretical approach towards the identification of cleavage-determining amino acid motifs of the 20 S proteasome. J Mol Biol 1999;286:1251–65.

30. Lode HN, Dreier T, Xiang R, et al. Gene therapy with a single chain interleukin 12 fusion protein induces T cell-dependent protective immunity in a syngeneic model of murine neuroblastoma. Proc Natl Acad Sci U S A 1998;95:2475–80.

31. Lode HN, Xiang R, Varki NM, et al. Targeted interleukin-2 therapy for spontaneous neuroblastoma metastases to bone marrow. J Natl Cancer Inst 1997;89:1586–94.

32. Lode HN, Xiang R, Dreier T, et al. Natural killer cell-mediated eradication of neuroblastoma metastases to bone marrow by targeted interleukin-2 therapy. Blood 1998;91:1706–15.

33. Rosenberg SA, Yang JC, Restifo NP. Cancer immunotherapy: moving beyond current vaccines. Nat Med 2004;10:909–15.

34. Krieg AM. CpG motifs in bacterial DNA and their immune effects. Annu Rev Immunol 2002;20:709–60.

35. Krieg AM. Development of TLR9 agonists for cancer therapy. J Clin Invest 2007;117:1184–94.

36. Liu YJ. IPC: professional type 1 interferon-producing cells and plasmacytoid dendritic cell precursors. Annu Rev Immunol 2005;23:275–306.

37. Bergman PJ, Camps-Palau MA, McKnight JA, et al. Development of a xenogeneic DNA vaccine program for canine malignant melanoma at the Animal Medical Center. Vaccine 2006;24:4582–5.

38. Yamano T, Kaneda Y, Hiramatsu SH, et al. Immunity against breast cancer by TERT DNA vaccine primed with chemokine CCL21. Cancer Gene Ther 2007;14:451–9.

39. Janssen EM, Lemmens EE, Wolfe T, et al. CD4+ T cells are required for secondary expansion and memory in CD8+ T lymphocytes. Nature 2003;421:852–6.

40. Fest S, Huebener N, Bleeke M, et al. Survivin minigene DNA vaccination is effective against neuroblastoma. Int J Cancer 2009;125:104–14.

41. Goldberg SM, Bartido SM, Gardner JP, et al. Comparison of two cancer vaccines targeting tyrosinase: plasmid DNA and recombinant αvirus replicon particles. Clin Cancer Res 2005;11:8114–21.

42. Orlandi F, Venanzi FM, Concetti A, et al. Antibody and CD8+ T cell responses against HER2/neu required for tumor eradication after DNA immunization with a Flt-3 ligand fusion vaccine. Clin Cancer Res 2007;13:6195–203.

43. Mescher MF, Curtsinger JM, Agarwal P, et al. Signals required for programming effector and memory development by CD8+ T cells. Immunol Rev 2006;211:81–92.

44. Xu S, Koski GK, Faries M, et al. Rapid high efficiency sensitization of CD8+ T cells to tumor antigens by dendritic cells leads to enhanced functional avidity and direct tumor recognition through an IL-12-dependent mechanism. J Immunol 2003;171:2251–61.

45. Hsieh CS, Macatonia SE, Tripp CS, et al. Development of TH1 CD4+ T cells through IL-12 produced by Listeria-induced macrophages. Science 1993;260:547–9.

46. Cochlovius B, Stassar MJ, Schreurs MW, Benner A, Adema GJ. Oral DNA vaccination: antigen uptake and presentation by dendritic cells elicits protective immunity. Immunol Lett 2002;80:89–96.

47. Sabel MS, Arora A, Su G, et al. Generation of a tumor-specific systemic response after intratumoral injection of IL-12 and IL-18-loaded polylactic acid microspheres. J Immunother 2007;30:808–16.

48. Zheng R, Cohen PA, Paustian CA, et al. Paired toll-like receptor agonists enhance vaccine therapy through induction of interleukin-12. Cancer Res 2008;68:4045–9.

49. Hueman MT, Stojadinovic A, Storrer CE, et al. Analysis of naive and memory CD4 and CD8 T cell populations in breast cancer patients receiving a HER2/neu peptide (E75) and GM-CSF vaccine. Cancer Immunol Immunother 2007;56:135–46.

Downloaded from mct.aacrjournals.org on January 16, 2021. © 2009 American Association for Cancer Research.

Published OnlineFirst August 11, 2009; DOI: 10.1158/1535-7163.MCT-09-0107

AACR American Association for Cancer Research

Molecular Cancer Therapeutics

Xenogeneic immunization with human tyrosine hydroxylase DNA vaccines suppresses growth of established neuroblastoma

Nicole Huebener, Stefan Fest, Kerstin Hilt, et al.

Mol Cancer Ther 2009;8:2392-2401. Published OnlineFirst August 11, 2009.

Updated version Access the most recent version of this article at: doi:10.1158/1535-7163.MCT-09-0107

Cited articles This article cites 49 articles, 18 of which you can access for free at: http://mct.aacrjournals.org/content/8/8/2392.full#ref-list-1

E-mail alerts Sign up to receive free email-alerts related to this article or journal.

Reprints and Subscriptions To order reprints of this article or to subscribe to the journal, contact the AACR Publications Department at pubs@aacr.org.

Permissions To request permission to re-use all or part of this article, use this link http://mct.aacrjournals.org/content/8/8/2392. Click on "Request Permissions" which will take you to the Copyright Clearance Center's (CCC) Rightslink site.

Downloaded from mct.aacrjournals.org on January 16, 2021. © 2009 American Association for Cancer Research.